PEOPLE'S DEMOCRATIC REPUBLIC OF ALGERIA
الجمهورية الجزائرية الديمقراطية الشعبية

MINISTRY OF HIGHER EDUCATION
AND SCIENTIFIC RESEARCH

HIGHER SCHOOL IN APPLIED SCIENCES
–T L E M C E N–

المدرسة العليا في العلوم التطبيقية
École Supérieure en
Sciences Appliquées

وزارة التعليم العالي والبحث العلمي

المدرسة العليا في العلوم التطبيقية
- تلمسان -

A Thesis Presented in Partial Fulfillment of the Requirements For

The Degree of Master

Department : Second Cycle
Specialization : Automation

Submitted by : MAKHALDI Mohamed Islam

ALAMI Mohamed Nadir

Thesis Title

Modeling and Simulation of a Proportional Pneumatic Valve with Positioner

Date : 23 June, 2026
before the jury composed of :

Dr.GHOUALIAmel	MCA	ESSATlemcen	President
Dr.Didi Ibtissem	MCA	ESSATlemcen	Examiner1
Pr.H.HadjAbdelkader	Professor	Evry Paris Sarclay University	Examiner2
Dr.S.M.Abdi	MCA	ESSATlemcen	Supervisor
Pr. B. Cherki	Professor	ESSA Tlemcen	Co-Supervisor

Academic Year : 2025 / 2026


بسم الله الرحمن الرحيم

Dedication

As this journey comes to an end, I find myself reflecting on how truly lucky I have been. It only deepens my gratitude to God for all the opportunities He placed in my path, all the chances He provided throughout my life, and for blessing me with my beloved family and the friends I encountered along the way. Words cannot repay their kindness, but this is the least I can offer.

To my friend, ALAMI Mohamed Nadir, with whom I began and completed this entire academic path. Thank you for your reliability, hard work, and the shared moments that made this journey memorable. I am incredibly glad to finish this chapter alongside you.

To my parents — for your endless efforts, immense patience, and unconditional love. Thank you for believing in me even when I lost faith in myself. This work, and every success I achieve, belongs entirely to you.

To my grandparents — whose prayers and guidance have been the bedrock of my success. Thank you for your unconditional love and for always standing by my side.

To my aunt — with deepest gratitude for the love, support, and guidance you have always shown me. I am incredibly fortunate to have you by my side.

To my brothers — thank you for all the good moments, the help, and the love.

To my cousins — thank you for your help, your mentorship, and for being role models worth looking up to.

To my dear maternal and paternal uncles and aunts — thank you for all the love, support, guidance, and kindness you have always shown me.

To all my educators — from my first days in primary school to my final days at university, thank you for your tireless efforts, your advice, and for sharing your knowledge so generously. Every step I took was built on what you gave me.

To my dear friends — those with whom I shared laughs, hardships, and struggles alike. To those who supported and stood by me, thank you for the company, the good moments, the memories, and the laughter. Your presence made the journey so much easier.

ISLAM

Reflecting on the journey that led to this point brings a deep sense of accomplishment. While the path had its share of challenges and demanding moments. As I reach the culmination of this academic chapter, I am incredibly grateful for the experiences that have shaped these years. It is an honor to dedicate this work to the most important people in my life, whose backing has been invaluable :

To my friend, Makhaldi Mohamed Islam, with whom I began and completed this entire academic path. Thank you for your reliability, hard work, and the shared moments that made this journey memorable. I am incredibly glad to finish this chapter alongside you.

To my brothers, for your motivation, and for always having my back throughout this demanding process.

To my grandfather and grandmother, your presence is a constant source of pride and inspiration.

To my teachers and professors, for your invaluable mentorship, patience, and dedication. Your guidance and the knowledge you shared were essential to making this achievement possible.

To my friends, for the shared laughs, breaks, and constant motivation that kept me grounded and moving forward.

To my mother, for your unconditional love, patience, and endless encouragement. Thank you for always believing in me and for being a constant source of strength throughout my studies.

To my father, for your support. Your reassurance has been vital to my success.

To my entire family, for always providing a solid foundation of support. NADIR

Acknowledgment

We extend our deepest gratitude to M. ABDI Sidi-Mohammed, our esteemed supervisor, whose expertise, mentorship, and unwavering support have been indispensable in shaping both this research and our academic journey. From guiding us through the intricacies of our project to offering invaluable insights, Mr. Abdi's continuous efforts have played a pivotal role in our success.

We would like to express our sincere appreciation to Mr. Cherki Brahim for providing us with essential information and insights, and to Mr. MESSIRDI for his invaluable guidance and support.

We are also deeply grateful to the members of the jury, Professor Hicham HadjAbdelkader,Dr. GHOUALI Amel and Dr Didi Ibtissem,for their time and valuable evaluation of this work. A special note of thanks is dedicated to Dr. Oudjamaa Farid, he was always present with us throughout our journey, offering continuous assistance, guidance, and support in various ways.

Our thanks also go to Mr. Belarousi, who consistently encouraged us, as well as to all of the school staff, whose support has been invaluable to us.

We also wish to extend our sincere thanks to Mr. Abde Ellatif for his constant assistance and cheerful disposition at the laboratory, which have been a source of motivation throughout these months of work.

Finally, we extend our heartfelt gratitude to all who have supported us in this endeavor, including professors, classmates, friends, and everyone who has contributed to this project.

Abstract

This study presents a comprehensive investigation into the modeling, system identification, and robust control design of an electro-pneumatic valve positioning system, with the objective of enhancing precision and reliability in industrial automation applications. The research begins with a foundational examination of industrial valve principles, classifications, and operating mechanisms, highlighting their indispensable role in fluid flow regulation across diverse process sectors. The historical trajectory of valve positioners is traced from early mechanical linkages and force-balance pneumatic devices to modern digital and smart positioners equipped with on-board diagnostics and fieldbus communication. Central to this work is the development of analytical transfer-function models for the double-acting pneumatic cylinder, the directional control valve, and the solenoid coil assembly, capturing the dominant dynamics that govern the electro pneumatic positioning loop. To accommodate the inherent nonlinearities of the physical plant ,including compressible airflow, mechanical friction, and valve hysteresis, a closed loop system identification approach is adopted, driven by a persistently exciting signal generated by an STM32 microcontroller. The results demonstrate the efficacy of the proposed modeling and identification framework as a foundation for high fidelity control design. This research contributes to the advancement of automated process instrumentation by establishing a structured methodology for the analysis and optimization of electro-pneumatic positioners, while paving the way for future developments in intelligent valve control and predictive diagnostics.

Résumé

Cette étude présente une analyse approfondie de la modélisation, de l'identification de systèmes et de la conception de commandes robustes d'un système de positionnement de vanne électropneumatique, dans le but d'améliorer la précision et la fiabilité des applications d'automatisation industrielle.

La recherche débute par un examen fondamental des principes, des classifications et des mécanismes de fonctionnement des vannes industrielles, mettant en évidence leur rôle indispensable dans la régulation du débit des fluides à travers divers secteurs industriels. L'évolution historique des positionneurs de vannes est retracée, depuis les premières liaisons mécaniques et les dispositifs pneumatiques à équilibre de forces jusqu'aux positionneurs numériques et intelligents modernes, équipés de diagnostics embarqués et de communication par bus de terrain.

Au cœur de ce travail se trouve le développement de modèles analytiques de fonctions de transfert pour le vérin pneumatique à double effet, le distributeur et l'ensemble bobine-solénoïde, capturant la dynamique dominante qui régit la boucle de positionnement électropneumatique. Pour s'adapter aux nonlinéarités inhérentes au système physique — notamment le débit d'air compressible, le frottement mécanique et l'hystérésis de la vanne —, une approche d'identification de système en boucle fermée est adoptée, pilotée par un signal d'excitation persistante généré par un microcontrôleur STM32.

الملخص

تُقدم هذه الدراسة بحثًا شاملًا في نمذجة نظام تحديد موضع الصمام الكهروبنيوماتيكي (الكهروهوائي)، وتحديد النظامتُقدم هذه الدراسة بحثًا شاملًا في نمذجة نظام تحديد موضع الصمام الكهروبنيوماتيكي، وتحديد النظام، وتصميم التحكم المتين، بهدف تعزيز الدقة والموثوقية في تطبيقات الأتمتة الصناعية.

يبدأ البحث بفحص أساسي لمبادئ الصمامات الصناعية، وتصنيفاتها، وآليات تشغيلها، مع تسليط الضوء على دورها الذي لا غنى عنه في تنظيم تدفق السوائل والغازات عبر قطاعات العمليات المختلفة. كما يتتبع البحث المسار التاريخي لمحددات مواضع الصمامات، بدءًا من الوصلات الميكانيكية المبكرة وأجهزة التوازن الهوائي للقوى، وصولاً إلى محددات المواضع الرقمية والذكية الحديثة المجهزة بأنظمة تشخيص مدمجة وبروتوكولات اتصالات ناقل المجال.

ويتمثل المحور الأساسي لهذا العمل في تطوير نماذج تحليلية لـ دوال التحويل لكل من الأسطوانة النيوماتيكية ثنائية الفعل، وصمام التحكم التوجيهي، ومجموعة الملف اللولبي، مما يتيح التقاط الديناميكيات المهيمنة التي تحكم حلقة التحديد الكهروبنيوماتيكية. ولمعالجة الخصائص اللاخطية المتأصلة في النظام الفيزيائي بما في ذلك تدفق الهواء القابل للانضغاط، والاحتكاك الميكانيكي، والتباطؤ الخاص بالصمام تم اعتماد نهج لتحديد النظام في حلقة مغلقة، يتم توجيهه بواسطة إشارة إثارة مستمرة تم توليدها عبر متحكم دقيق من نوع إس تي إم ٣٢.

تُظهر النتائج فعالية إطار النمذجة والتحديد المقترح كقاعدة أساسية لتصميم أنظمة تحكم عالية الدقة. ويساهم هذا البحث في تطوير أجهزة العمليات المؤتمتة من خلال وضع منهجية منظمة لتحليل وتحسين محددات المواضع الكهروبنيوماتيكية، مع تمهيد الطريق للتطورات المستقبلية في التحكم الذكي في الصمامات والتشخيصات التنبؤية.

Table of Contents

List of Figures **13**

List of Tables **14**

Abbreviation **14**

Introduction **15**

1 Generalities on Industrial Valves and Pneumatic Actuators **18**

1.1 Introduction 18
1.2 Definition and Classification of Valves 18
1.3 Historical Evolution of Fluid Control Technology 19
1.4 Classification of Valves 20
1.4.1 Classification According to Function 20
1.4.2 Classification Based on Mechanical Motion 22
1.5 Control Valves 22
1.6 Pneumatic Actuator Valve 23
1.7 Pneumatic Cylinders 24
1.7.1 Classification of Pneumatic Cylinders 24
1.8 Conclusion 25

2 System Description and Mathematical Structure 26
2.1 Introduction to Valve Positioners 26
2.2 Operating Principle of Valve Positioners 26
2.3 Types of Valve Positioners 27
2.3.1 Pneumatic Positioners 27
2.3.2 Digital and Smart Positioners 28
2.3.3 Smart Valve Positioners and Intelligent Systems 29
2.4 Operational Architecture of the Analog Electro-Pneumatic (E/P) Positioner 29
2.4.1 Mechanical and Pneumatic Sub-Assemblies 30
2.5 Electro-Pneumatic (I/P) Transducers 31
2.5.1 Conventional Flapper-Nozzle Mechanism 32
2.5.2 Flapper Nozzle Amplifier 32
2.5.3 Air Relay 33
2.6 Mathematical Model Structure 34
2.7 Conclusion 36

3 System Identification and Modelling of the Electro-Pneumatic Positioning System 37
3.1 Introduction 37
3.2 Simplified Model Structure Selection 38
3.2.1 AutoRegressive with Exogenous Input (ARX) Model . . . 38
3.2.2 AutoRegressive Moving Average with Exogenous Input (ARMAX) Model 39
3.3 System Identification via Structured Process Models 39
3.3.1 Mathematical Structure of the `idproc` Class 40
3.3.2 Estimation Theory and Optimization Mechanics 41
3.4 Transfer Function Identification 42
3.5 Validation of Open Loop 47
3.5.1 Open-Loop Model Validation 47
3.6 Conclusion 50
3.7 Fixed-Structure H_∞ Optimal Tuning via `hinfstruct` 50
3.7.1 Introduction 50

3.7.2 Theoretical Framework and Generalized Plant Synthesis . 51
3.7.3 Application to the Proposed Model 52
3.7.4 Simulation Results 54
3.7.5 Experimental Results of the H_∞-Tuned PID Controller . . 54
3.8 Conclusion 55

conclusion **56**

List of Figures

1.1 Gate vs Globe Valves. 19
1.2 One-way (non-return) valve. 20
1.3 Throttling valve. 21
1.4 Shut-off / shut-down valve. 21
1.5 Rectilinear (linear) valve. 22
1.6 Rotary motion valve. 22
1.7 Quarter-turn valve. 22
1.8 Control valve assembly. 23

2.1 Industrial valve positioner overview. 27
2.2 Pneumatic valve positioner. 28
2.3 Digital smart valve positioner. 28
2.4 Smart valve positioner with integrated diagnostics. 29
2.5 Mechanical and pneumatic sub-assemblies of the EP100 positioner. 31
2.6 Conventional flapper-nozzle mechanism of an I/P transducer. . . 32
2.7 Nozzle flapper system with amplifier 33

3.1 identification close loop 43
3.2 Comparison between measured and simulated position responses [1]. 45
3.3 Simulink block diagram used for the model validation 47
3.4 Open loop controle signals 48

3.5 Open-loop model validation : measured vs. simulated position responses 49
3.6 Simulation results of position 54
3.7 Real results of position 55

List of Tables

3.1 Structural Class Definers for the `idproc` Model Space 41

Abbreviation

Acronyme	Signification
ASME	American Society of Mechanical Engineers
ANSI	American National Standards Institute
NRV	Non-Return Valve
PRV	Pressure Relief Valve
ESD	Emergency Shutdown System
NPS	Nominal Pipe Size
DN	Nominal Diameter (Diamètre Nominal)
PTFE	Polytetrafluoroethylene
CRA	Corrosion-Resistant Alloy

General Introduction

The automation of fluid power systems represents a cornerstone of modern industrial engineering, where the precise regulation of pressure, flow, and mechanical displacement governs the reliability of process operations across the petrochemical, manufacturing, and energy sectors. At the heart of these systems lie valves and their associated actuation architectures, which translate control logic into physical action. This thesis presents a comprehensive investigation into electro-pneumatic valve control systems, progressing from the foundational mechanics of industrial valves to the robust control design of a nozzle-flapper pneumatic positioner. The study begins by establishing the theoretical groundwork, examining valve classifications by function, mechanical motion, and size, alongside the operating principles of manual and control valves and the pneumatic cylinders that drive them. Building upon this foundation, the work explores the role of valve positioners as closed-loop intermediaries that compensate for mechanical non-idealities such as stiction, deadband, and hysteresis, tracing their evolution from early mechanical linkages to modern smart digital devices. Central to the investigation is the mathematical modeling of the double-acting cylinder, directional control valve, and solenoid assembly, from which governing transfer functions are derived. The thesis then advances toward system identification, employing a closed-loop approach driven by an STM32 microcontroller to extract a linear approximation of the inherently nonlinear plant dynamics, accounting for compressible airflow, friction, and valve hysteresis. The identified model is validated against experimental hardware

responses, with residual discrepancies attributed to unmodeled nonlinearities. Ultimately, these uncertainties motivate the development of a robust control strategy, providing a complete trajectory from passive mechanical components to embedded, high-fidelity closed-loop control.

CHAPITRE 1

Generalities on Industrial Valves and Pneumatic Actuators

1.1 Introduction

Valves serve as the critical final control elements within fluid power and process piping networks, facilitating the precise regulation, isolation, and directional control of multi-phase media. A thorough understanding of the kinematic mechanisms, fluid dynamics, and seating designs governing these devices is a prerequisite for optimal system selection and asset lifecycle management. This chapter provides a systematic overview of valve classifications, mechanical operating principles, and their functional roles across industrial sectors, tracing the historical evolution from primitive manual regulation to the highly automated actuation architectures of modern process industries. It also examines pneumatic actuator systems—including cylinder classifications and fail-safe architectures—providing the technical baseline for the closed-loop control designs developed in subsequent chapters.

1.2 Definition and Classification of Valves

A valve is a precision-engineered mechanical assembly designed to isolate, modulate, direct, or blend process media by varying the fluid flow area through mechanical displacement of an internal closure member. The operational enve-

lope of modern industrial valves spans several orders of magnitude :

- **Dimensional Scale :** Nominal pipe sizes from 0.5 in (DN 15) to over 48 in (DN 1200).
- **Mass Profiles :** From less than 1 lb (0.45 kg) up to heavy castings exceeding 10 tons (9,070 kg).
- **Pressure Regimes :** From ultra-high vacuum up to severe-service limits exceeding 13,000 psi (897 bar).

Primary industrial typologies—categorized by closure mechanics—encompass gate, plug, ball, butterfly, check, globe, and pressure-relief configurations. To maintain structural and chemical integrity, valves are fabricated from carbon steels, cast iron, polymers, brass, bronze, and corrosion-resistant alloys (CRAs) such as duplex stainless steel or Inconel. [2]

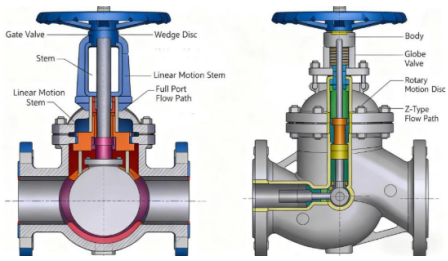


Figure 1.1 – Gate vs Globe Valves.

1.3 Historical Evolution of Fluid Control Technology

The development of fluid control mechanisms mirrors the trajectory of civil and mechanical engineering. The earliest paradigms of systematic flow regulation date to approximately 5000 BC, where Egyptian and Mesopotamian civilizations engineered sluice gates for irrigation. Greek and Roman engineers advanced these techniques by casting bronze plug cocks and executing sophisticated aqueduct networks using gravity-fed hydrostatic principles. The Renaissance catalyzed a shift toward mechanical complexity : da Vinci's technical treatises introduced the automatic check valve and the hinged flap valve, establishing foundational logic for passive directional control.

The modern evolution of valves began with the Industrial Revolution. Steam engines pioneered by Newcomen and Watt introduced thermodynamic challenges that drove the transition from simple wooden or brass plugs to heavy-duty cast-iron safety relief and globe valves. Throughout the 19th and 20th centuries, the rise of petrochemistry and automated municipal networks standardized component interchangeability, accelerating the development of high-integrity metallurgy and complex actuation architectures. [2]

1.4 Classification of Valves

1.4.1 Classification According to Function

One-Way Valves (Non-Return Valves)

In applications where unidirectional fluid transport is critical, non-return valves (NRVs) mitigate backflow by actuating when suction-side pressure surpasses discharge-side pressure. Conventional NRVs rely on mechanically actuated components; although static alternatives with no moving parts exist and offer theoretical advantages, their industrial adoption remains disproportionately low. [3, 4]



Figure 1.2 – One-way (non-return) valve.

Throttling Valves

Throttling valves modulate flow, temperature, or pressure and can be adjusted to any position within their stroke—from fully open to fully closed—allowing them to serve both as modulating and shut-off devices. Manual configurations use handwheels or levers; automated systems rely on pneumatic, hydraulic, or electric actuators. A prominent subcategory is the pressure regulator, which manages upstream or downstream pressure by dynamically adjusting the valve orifice. [5, 6, 7]

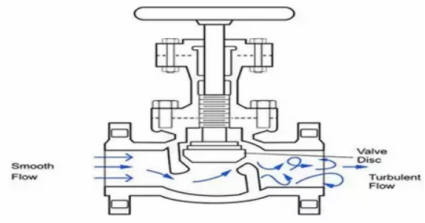


Figure 1.3 – Throttling valve.

Shut-off / Shut-down Valves

Shut-off valves (block or isolation valves) either permit or completely obstruct media passage. Typical architectures include gate, plug, ball, and tank bottom configurations. They are vital to Emergency Shutdown Systems (ESD), enabling rapid process isolation during critical failures. A specialized subset is the Pressure Relief Valve (PRV), categorized into relief valves (liquid overpressurization) and safety valves (gas or vapor hazards).



Figure 1.4 – Shut-off / shut-down valve.

1.4.2 Classification Based on Mechanical Motion

Valves are fundamentally categorized by the kinematic profile of their closure members :

— **Linear Motion Valves :** The closure member moves in a straight line. Examples : gate, globe, diaphragm, and pinch valves. Globe valves excel at throttling ; gate valves provide an unobstructed flow path.

— **Rotary Motion Valves :** The closure element travels along an angular or circular trajectory. Examples : butterfly, ball, and plug valves. Their mechanical advantage yields compact designs and faster actuation.

— **Quarter-Turn Valves :** A specific subset of rotary valves requiring a precise 90° rotation to transition between fully closed and fully open states, ideal for emergency isolation and high-cycle processes.

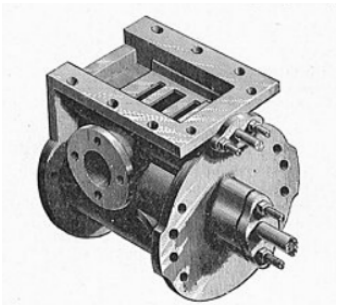


Figure 1.5 – Rectilinear (linear) valve.



Figure 1.6 – Rotary motion valve.



Figure 1.7 – Quarter-turn valve.

1.5 Control Valves

A control valve is a throttling device integrated with an actuation system and engineered for operation within a closed-loop control architecture. The actuator transduces external pneumatic, hydraulic, or electronic signals into the mechanical thrust or torque required to modulate the obturator's position. Within a standard process loop (sensor → controller → final control element), the valve is the terminal component executing the controller's logic. By dynamically adjusting the flow area in response to real-time feedback, it regulates pressure,

temperature, and mass flow rate. Common configurations include globe, butterfly, ball, and eccentric plug designs, each selected based on gain characteristics and the thermodynamic requirements of the process.



Figure 1.8 – Control valve assembly.

1.6 Pneumatic Actuator Valve

Pneumatic actuators convert the potential energy of compressed air into proportional linear or rotary mechanical displacement. An industrial compressor charges a reservoir to supply high-pressure air through regulation manifolds to the actuator chamber. When properly maintained, pneumatic cylinders exhibit minimal parasitic friction (typically less than 5% of total energy input) and exceptional thermal resilience (−200°C to 250°C). However, two key system-level constraints apply :

— **Compressibility Effects :** The low bulk modulus of compressed air makes these actuators susceptible to stick-slip and velocity fluctuations under variable loads, requiring sophisticated closed-loop digital positioners for high-precision positioning.

— **Force Density Limitations :** Standard industrial supply pressures (4–8 bar) yield lower force density than hydraulic alternatives, requiring larger piston areas to deliver equivalent thrust ($F = P \cdot A$).

1.7 Pneumatic Cylinders

Pneumatic cylinders translate compressed-air energy into precise linear thrust. In valve systems, their displacement clamps closure elements against high fluid pressures, tilts or rotates heavy internal assemblies, and meters flow rates. They are the primary physical link between the automated control signal and the mechanical regulation of the pipeline.

1.7.1 Classification of Pneumatic Cylinders

Classification Based on Duty Cycle and Structural Load

- **Light-Duty :** Aluminum alloys or polymers, for high-speed, low-force applications.
- **Medium-Duty :** Brass or thin-walled steel, balancing strength and weight for standard automation.
- **Heavy-Duty :** Cast iron or thick-walled carbon steel, for severe environments and high pressures.

Classification Based on Fluid Action and Return Mechanics

- **Single-Acting :** Pneumatic pressure drives one direction ; return is passive via spring, gravity, or process load. Used in fail-safe valve designs (Fail-Closed / Fail-Open).
- **Double-Acting :** Driven bi-directionally by alternating pressure across the piston.
  - *Single-Rod :* Asymmetric pressure area—higher thrust on extension ($F_{ext} = P \times A_{piston}$) than retraction ($F_{ret} = P \times [A_{piston} - A_{rod}]$).
  - *Double-Rod :* Symmetrical rods on both sides, yielding equal force and velocity in both directions.

1.8 Conclusion

This chapter established the technical foundation for the control work developed in subsequent chapters. Industrial valves were examined across their principal classification axes functional role, closure mechanics, and material construction highlighting how each typology addresses specific process constraints. The historical survey traced the progression from primitive sluice gates to precision-engineered control assemblies, contextualizing the demands that modern process industries place on fluid regulation hardware. The discussion of pneumatic actuators and cylinder architectures revealed the core trade-offs inherent to compressed-air systems : thermal resilience and low friction offset by compressibility-induced instability and limited force density relative to hydraulic alternatives. These limitations directly motivate the need for closed-loop digital positioners and robust control strategies—the central focus of the chapters that follow.

CHAPITRE 2

System Description and Mathematical Structure

2.1 Introduction to Valve Positioners

This chapter examines the critical function of valve positioners within automated control architectures. As specialized intermediaries, positioners translate low power output signals from a process controller into high power pneumatic or hydraulic adjustments to the actuator, ensuring the valve reaches the exact displacement commanded by the control logic. A cornerstone of this technology is the integration of mechanical or electronic position feedback, which creates a localized control loop to optimize process efficiency.

Beyond signal translation, the primary utility of a positioner lies in its ability to mitigate mechanical non idealities. Industrial valves often encounter static friction (stiction), deadband, and hysteresis, all of which can severely degrade control accuracy and lead to process oscillations. By monitoring the actual stem position relative to the input signal, the positioner dynamically compensates for these forces, providing the necessary force to overcome friction and ensuring high fidelity positioning in demanding process loops. [8, 5]

2.2 Operating Principle of Valve Positioners

The fundamental operating principle of a valve positioner is based on negative feedback control. The device acts as a high gain comparator that continuously evaluates the command signal from the process controller (the "set-



Figure 2.1 – Industrial valve positioner overview.

point") against the physical displacement of the valve stem (the "process variable"). When a deviation, or error signal, is detected between the input command and the actual position, the positioner modulates its pneumatic output to the actuator. This pressurized air provides the necessary thrust or torque to reposition the valve until the error is nulled.

Beyond basic positioning, the device functions as a pneumatic power amplifier. It accepts a low volume control signal and utilizes a separate high pressure supply to deliver the volumetric flow required for rapid actuation. In modern instrumentation, positioners often feature integrated I/P (Current to Pressure) transducers, enabling them to convert standard 4–20 mA electronic signals directly into proportional pneumatic outputs. Advanced "smart" positioners can even execute localized PID control logic by processing raw sensor data, thereby reducing the computational load on the main Distributed Control System (DCS). [9, 10]

2.3 Types of Valve Positioners

2.3.1 Pneumatic Positioners

The evolution of fluid power led to the development of pneumatic valve positioners, which became the industrial standard for several decades. These devices operate on a force balance principle, where a pneumatic command signal (traditionally 3–15 psi) is balanced against a feedback spring connected

to the valve stem. Any change in the signal pressure or the valve's physical position creates an imbalance in the internal relay or flapper-nozzle assembly, causing the positioner to adjust the air supply to the actuator until equilibrium is restored. These positioners are primarily utilized alongside pneumatic actuators to provide robust, reliable control in environments where electrical components might pose a safety risk or where high pressure air is readily available.



Figure 2.2 – Pneumatic valve positioner.

2.3.2 Digital and Smart Positioners

Digital positioners have transformed valve instrumentation from simple transducers into intelligent field devices. By replacing analog mechanisms with electronic sensors and digital signal processing, they execute high-fidelity control and integrate seamlessly with central systems via protocols like HART or Profibus. Beyond precise positioning, this digital architecture enables real-time on-board diagnostics—tracking friction, cycle counts, and wear—to facilitate predictive maintenance, while automated self-calibration significantly reduces commissioning time.



Figure 2.3 – Digital smart valve positioner.

2.3.3 Smart Valve Positioners and Intelligent Systems

"Smart" or "intelligent" valve systems represent the pinnacle of modern control technology by pairing integrated process sensors with a high-performance microprocessor. By calculating real-time mass or volumetric flow rates directly from internal pressure and temperature data, these units function as self-contained, autonomous loops. This decentralized architecture modulates the obturator locally to maintain setpoints, effectively offloading computational tasks from the central Distributed Control System (DCS) so it can focus on higher-level plant optimization. Additionally, this embedded intelligence provides a robust framework for predictive diagnostics and safety management in critical environments.



Figure 2.4 – Smart valve positioner with integrated diagnostics.

2.4 Operational Architecture of the Analog Electro-Pneumatic (E/P) Positioner

The analog positioner serves as the critical interface for the precise modulation of pneumatic actuators, utilising a standardised 4–20 mA current loop. In this architecture, the positioner functions as a closed-loop controller that processes electronic inputs into mechanical displacement. Taking the EP100 series

as a modular archetype, the operational sequence is as follows :

— **Signal Processing :** The electronics unit receives the 4–20 mA signal, with the input range optimised via dip switches (S4–S7). An adjustable time constant (P5) in Circuit 10 facilitates signal damping to prevent system instability.

— **Transduction :** The processed signal enters the analog control circuit (11), where gain — modulated by potentiometer P4 — governs the drive current for the I/P (Current-to-Pressure) Module (12).

— **Pneumatic Amplification :** The I/P module regulates a single or double-acting pneumatic amplifier (14). Utilising a supply pressure (P_s) of 1.4 to 6 bar, the amplifier generates the necessary output pressures to actuate the valve.

— **Feedback & Calibration :** The physical displacement (x) is monitored by a high-precision conductive plastic potentiometer (15). The system is calibrated via the Zero (P3) and Span (P2) potentiometers, ensuring the electrical input aligns perfectly with the mechanical stroke or rotation angle.

Integrated mechanical indicators (16) and optional limit switches (22) provide independent verification of valve status and alarm signalling, ensuring operational safety and diagnostic transparency.

[11] [12] [13]

2.4.1 Mechanical and Pneumatic Sub-Assemblies

The mechanical and pneumatic units of the EP100 are designed for high reliability and ease of field service. The **Amplifier** manages air delivery with specialised O-ring counts for single and double-acting control, while the **Pre-amplifier** handles initial signal boosting with a four seal protective array. The **I/P Module** acts as the system's electromechanical bridge, regulating pneumatic pilot signals based on electronic inputs. Finally, the **Feedback Unit** monitors the valve's actual position, translating mechanical movement back into the control loop. Each unit is modular, allowing for targeted replacement of O-rings and fastening hardware to maintain long-term operational integrity.

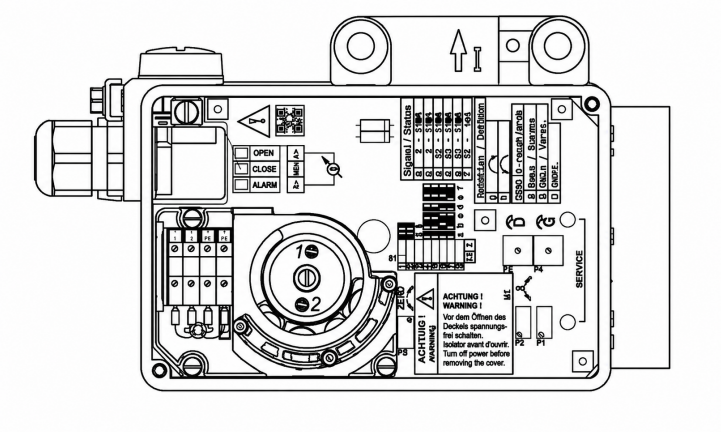


Figure 2.5 – Mechanical and pneumatic sub-assemblies of the EP100 positioner.

2.5 Electro-Pneumatic (I/P) Transducers

Current-to-Pressure (I/P) transducers are fundamental signal converters that facilitate the integration of electronic control systems with pneumatic final control elements. The device functions by linearly converting a standardised 4–20 mA current loop into a proportional pneumatic output, typically spanning 3–15 psi (21–103 kPa). To be effective in high-dynamic process loops, an I/P transducer must exhibit high volumetric efficiency — providing rapid charging of the actuator diaphragm while facilitating high-speed exhaust when the control signal is attenuated.

Beyond basic transduction, industrial-grade I/Ps must maintain high-fidelity performance under adverse environmental stressors, including mechanical vibration, thermal fluctuations, and corrosive or contaminated atmospheric conditions. While the flapper-nozzle assembly has remained the mechanical standard since the 1960s, contemporary designs have evolved to include solid-state components and advanced feedback mechanisms. These modern iterations prioritise low "steady-state" air consumption and enhanced resilience to particulate contamination, ensuring long-term reliability in severe service applications.

2.5.1 Conventional Flapper-Nozzle Mechanism

The traditional I/P transducer operates on a force-balance principle, utilising a coil-armature assembly to convert electrical current into mechanical displacement. The input current (4–20 mA) generates a magnetic field that exerts a proportional force on a pivoting beam, known as the flapper. This flapper is positioned in close proximity to a precision nozzle, which is supplied with constant air pressure.

The physical gap between the flapper and the nozzle orifice dictates the pneumatic backpressure (or pilot pressure) within the sensing line. As the flapper moves closer to the nozzle, it restricts the air escape, causing an increase in backpressure ; conversely, increasing the gap reduces the pressure. To ensure linear response and stability, many designs integrate a feedback bellows or a counter-spring. This component exerts a restoring force on the beam to counteract the magnetic pull, effectively nulling the error and ensuring the output pressure remains precisely proportional to the input current. [12, 14]

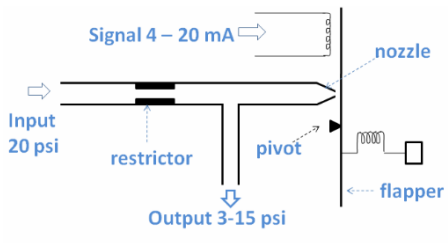


Figure 2.6 – Conventional flapper-nozzle mechanism of an I/P transducer.

2.5.2 Flapper Nozzle Amplifier

A pneumatic control system uses compressed air as its working medium, where information is transmitted through changes in air pressure, typically ranging from 0.2 to 1.0 bar (3–15 psi), to trigger control actions. A fundamental component of such systems is the flapper–nozzle amplifier, which transforms very small mechanical displacements, on the order of microns, into corresponding variations in air pressure. The basic structure of a flapper–nozzle amplifier is illustrated in Figure 2.11

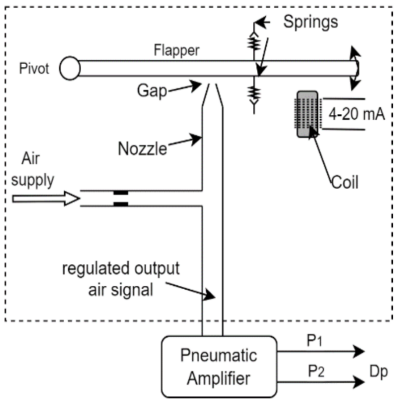


Figure 2.7 – Nozzle flapper system with amplifier

A constant air supply is applied to one end of the pipeline through a restriction orifice. At the opposite end, a nozzle and flapper arrangement is installed. The distance between the nozzle and flapper is controlled by the input signal. When the flapper moves closer to the nozzle, airflow through the nozzle is reduced, causing the pressure within the pipe to rise. Conversely, as the flapper moves farther from the nozzle, more air escapes and the pressure decreases. In the limiting case, when the nozzle is fully open (flapper far away), the output pressure equals atmospheric pressure. When the nozzle is completely blocked, the output pressure becomes equal to the supply pressure. [15]

2.5.3 Air Relay

A key limitation of the flapper–nozzle amplifier is its low air handling capacity, meaning the pressure variation it produces is too small for most practical applications unless it is amplified. To overcome this, an air relay is used downstream to increase the volume of air being controlled. The operating principle of the air relay can be understood from the schematic in Figure 2.12. The relay is connected directly to the supply line without an intermediate orifice. The output pressure from the flapper–nozzle amplifier (p2) is fed into the lower chamber of the relay, while a diaphragm is positioned at the top. Changes in p2 cause the diaphragm to move by a displacement y. A double-seated valve is attached to the diaphragm. When the nozzle pressure p2 rises due to a decrease in xi,

the diaphragm lifts upward, closing the vent line and opening a path between the supply line and the output, allowing more air to flow and increasing output pressure. When p2 drops, the diaphragm moves downward, closing the supply line and connecting the output to the vent, which reduces the output pressure. [16]

2.6 Mathematical Model Structure

To ensure a highly accurate dynamical system identification procedure, this section focuses on selecting an appropriate mathematical model structure for the cylindrical actuator system equipped with a pneumatic positioner. The primary objective is to derive the transfer function relating the input control signal to the final valve position.

System Variables and Signals

— **Input Signal** $u(t)$: Represents the control signal applied to the pneumatic positioner, utilizing a standard 4–20 mA current loop.
— **Piston Linear Position** $Y(t)$: Represents the physical displacement of the internal pistons within the actuator.
— **Rotary Position** $\theta(t)$: Measured from 0% to 100%, this variable represents the angular position of the rotary actuator, which directly mirrors the linear position $Y(t)$.

Modeling Assumptions and Dynamics

Adopting this modeling approach significantly simplifies the mathematical identification process. However, selecting a precise model structure remains critical to achieving the optimal fit during experimental validation.

The coil directly regulates the nozzle-flapper gap, which subsequently dictates the velocity and direction of the double-acting cylinder. The relationship between the internal cylinder pressures and the piston position is defined in Equation (2.6.1).

Furthermore, the static characteristics of the double-acting valve can be determined via a force balance analysis. By neglecting hysteresis, a foundational equation can be established for both the extension and retraction of the cylinders. For simplicity during this analysis, the motion is assumed to be unidirectional, yielding the following dynamic equation of motion :

$$m\,\ddot{Y}(t) = D_p - F_n\,\dot{Y}(t) \tag{2.6.1}$$

where :

$$D_p = A_1 P_1 - A_2 P_2$$
$$F_n = K_n\,\dot{Y}$$

Here, F_n represents the nonlinear friction forces, and K_n denotes the viscous friction coefficient. Assuming equal piston areas ($A_1 = A_2 = A$), the relationship between the piston position and the cylinder's differential pressure (ΔP) is expressed in Equation (2.6.2) :

$$\frac{Y(s)}{\Delta P(s)} = \frac{A/K_n}{s\,(T_2 s + 1)} \tag{2.6.2}$$

where the time constant T_2 is defined as $T_2 = \dfrac{m}{K_n}$.

Pressure and Input Signal Relationship

The transfer function between the cylinder differential pressure and the current input signal (I) is approximated as a first-order dynamical system, given by Equation (2.6.3) :

$$\frac{\Delta P(s)}{I(s)} = \frac{k_g}{T_1 s + 1} \tag{2.6.3}$$

where T_1 is the system time constant, and k_g is the gain modeling the ratio between the nozzle-flapper gap and the differential pressure.[1]

Overall System Transfer Function

By substituting Equation (2.6.3) into Equation (2.6.2) and defining the total system gain k_s, the overall transfer function structure from the current control signal to the cylinder position is derived as Equation (2.6.4) :

$$\frac{Y(s)}{I(s)} = \frac{k_s}{s\,(T_2 s + 1)(T_1 s + 1)} \tag{2.6.4}$$

where the gain constant is defined as :

$$k_s = \frac{K_n \cdot k_g}{A} \tag{2.6.5}$$

[1]

2.7 Conclusion

This chapter provided a comprehensive foundation for understanding the operational principles and mathematical modeling of the nozzle-flapper pneumatic valve positioner system. Beginning with an overview of valve positioner technology, the evolution from early mechanical assemblies to modern smart devices was examined, highlighting the progressive improvements in precision, diagnostics, and system integration.

The operational architecture of the analog electro-pneumatic positioner was analyzed in detail, with particular focus on the EP100 series as a representative platform. The internal signal chain — from the 4–20 mA input through the I/P transduction stage to the final mechanical displacement — was systematically described, establishing the physical basis for the dynamic model developed in subsequent chapters.

CHAPITRE 3

System Identification and Modelling of the Electro-Pneumatic Positioning System

3.1 Introduction

This chapter addresses the mathematical characterisation of the electro-pneumatic valve positioning system through system identification techniques. Given the inherent nonlinearities of the physical plant — including compressible airflow dynamics, mechanical friction, and valve hysteresis — a purely analytical modelling approach presents significant practical limitations. The identification procedure therefore aims to derive a linear approximation of the dominant system dynamics around a selected operating point, suitable for control design purposes.

The chapter begins by reviewing the parametric model structures considered for identification, namely the ARX, ARMAX, Box-Jenkins, Output-Error, and Hammerstein models, with a discussion of the trade-offs each presents in terms of complexity, noise representation, and estimation tractability. A closed-loop identification approach is then adopted, driven by a persistently exciting input signal generated by the STM32 microcontroller. The resulting experimental data are used to estimate the parameters of a third-order closed-loop transfer function, from which the open-loop plant model is algebraically recovered. The chapter concludes with an open-loop hardware validation experiment, in which the identified model is compared against the physical system response under periodic square-wave excitation.

3.2 Simplified Model Structure Selection

Several parametric model structures are available for characterising the system dynamics, including the AutoRegressive with Exogenous Input (ARX), Auto-Regressive Moving Average with Exogenous Input (ARMAX), Output Error (OE), and Box-Jenkins (BJ) models. The selection of an appropriate model structure depends on the nature of the process, the characteristics of the disturbances acting upon it, and the intended application of the identified model. Each structure offers a distinct trade-off between model complexity, noise representation capability, and estimation tractability.

3.2.1 AutoRegressive with Exogenous Input (ARX) Model

The ARX model represents the most straightforward approach to incorporating an excitation signal. Furthermore, the parameter estimation procedure associated with the ARX model constitutes one of the most computationally efficient polynomial estimation techniques, as it reduces to the solution of a system of linear regression equations in closed form.

The ARX model structure can be written as :

$$y(k) = \frac{B(q)}{A(q)} \cdot u(k) + \frac{1}{A(q)} \cdot e(k) \tag{3.2.1}$$

where $y(k)$ denotes the system output at time k, $u(k)$ represents the input signal at time k, and $e(k)$ corresponds to the noise signal at time k. The polynomials $A(q)$ and $B(q)$ are functions of the forward shift operator q, with $A(q)$ governing the autoregressive dynamics and $B(q)$ relating the exogenous input to the output.

A key characteristic of the ARX structure is that the noise model shares the same denominator polynomial $A(q)$ as the process model. Consequently, any mismatch between the true noise dynamics and the assumed structure may introduce bias into the parameter estimates. Despite this limitation, the ARX model remains widely employed in practice due to its simplicity and its amenability to least-squares estimation, which yields a globally optimal solution in a single computational step.[17]

3.2.2 AutoRegressive Moving Average with Exogenous Input (ARMAX) Model

Unlike the ARX model, the ARMAX structure incorporates an explicit representation of disturbance dynamics through the introduction of a moving average polynomial $C(q)$. The ARMAX model is particularly advantageous in applications characterised by dominant disturbances entering early in the process, such as at the system input.

The ARMAX model structure is expressed as :

$$y(k) = \frac{B(q)}{A(q)} \cdot u(k) + \frac{C(q)}{A(q)} \cdot e(k) \tag{3.2.2}$$

where $C(q)$ is the moving average polynomial that shapes the spectral properties of the additive noise. The inclusion of $C(q)$ provides greater flexibility in modelling coloured noise sequences, making ARMAX more suitable than ARX when disturbances exhibit significant dynamic content.

However, the additional polynomial introduces a nonlinearity in the parameter estimation problem, since $C(q)$ appears in the noise term alongside $A(q)$, which also governs the process dynamics. As a result, parameter estimation for the ARMAX structure typically requires iterative optimisation methods, such as the prediction error minimisation framework, rather than the direct closed-form solution available for ARX models.[17]

3.3 System Identification via Structured Process Models

In practical industrial applications, such as the control of pneumatic valve positioners, traditional black-box identification methods (e.g., ARX, ARMAX, or unstructured state-space formulations) often yield high-order discrete-time transfer functions. While mathematically flexible, these polynomial coefficients lack direct physical meaning, rendering them difficult to validate against known plant characteristics or to utilize directly for analytical PID or Internal Model

Control (IMC) tuning.

To bridge the gap between experimental data and physical intuition, the MATLAB System Identification Toolbox provides a dedicated model class known as `idproc` (Process Models). The core paradigm of this framework is to fit low-order, continuous-time transfer functions parameterized exclusively by physically meaningful quantities : static gain, dominant time constants, damping ratios, natural frequencies, transport delays, and optional integrators or zeros.

3.3.1 Mathematical Structure of the `idproc` Class

The generic Single-Input Single-Output (SISO) continuous-time transfer function representation supported by the `idproc` class is bounded at three poles, one zero, one transport delay, and one free integrator. The fully expanded operational template is formulated as :

$$G(s) = \frac{K_p(1 + T_z s)}{s^\gamma(1 + T_{p1}s)(1 + T_{p2}s)(1 + T_{p3}s)} e^{-T_d s} \tag{3.3.1}$$

where the structural parameters are physically defined as follows :

— $K_p \in \mathbb{R}$: The steady-state open-loop plant gain.

— $T_{p1}, T_{p2}, T_{p3} \in \mathbb{R}^+$: Real-valued positive time constants representing dominant plant poles.

— $T_z \in \mathbb{R}$: A numerator time constant defining a system zero, capable of capturing non-minimum phase behavior (inverse response) if $T_z < 0$, or overshoot characteristics if $T_z > 0$.

— $T_d \in \mathbb{R}^+$: The continuous transport lag or dead time.

— $\gamma \in \{0, 1\}$: A structural switch defining the absence ($\gamma = 0$) or presence ($\gamma = 1$) of a free integrator, typical of positioning or liquid level dynamics.

The Structural Type Code

The toolbox identifies these configurations through a standardized, compact alphanumeric type code. The structural configuration is parsed using the format **P*n*[U][Z][D][I]**, where $n \in \{1, 2, 3\}$ denotes the total number of poles. The

operational meanings of the structural modifiers are summarized in Table 3.1.

Table 3.1 – Structural Class Definers for the `idproc` Model Space

Code	Physical Meaning	Associated Parameters
`P1, P2, P3`	Total number of system poles (n)	T_{p1}, T_{p2}, T_{p3}
`U`	Replaces a real pole pair with an underdamped pair	T_w, ζ
`Z`	Appends a numerator zero to the plant structure	T_z
`D`	Enforces a non-negative transport delay (dead time)	T_d
`I`	Introduces an open-loop integrator element ($1/s$)	$\gamma = 1$

Under this convention, a `P1D` denotes a classic First-Order Plus Dead Time (FOPDT) model ($G(s) = \frac{K_p}{1+T_{p1}s}e^{-T_d s}$), whereas a `P3U` model denotes an underdamped second-order pair coupled with an additional real pole, expressed mathematically as :

$$G_{P3U}(s) = \frac{K_p}{(1 + 2\zeta T_w s + T_w^2 s^2)(1 + T_{p3}s)} \tag{3.3.2}$$

3.3.2 Estimation Theory and Optimization Mechanics

The routine `procest` executes parameter estimation within a prediction-error framework. Let θ define the vector of unknown physical parameters to be estimated :

$$\theta = \begin{bmatrix} K_p & T_w & \zeta & T_{p3} & T_z & T_d \end{bmatrix}^T \in \mathbb{R}^d \tag{3.3.3}$$

Given a set of N sampled input-output data pairs $Z^N = \{[u(t_k), y(t_k)]\}_{k=1}^N$ collected at a sampling interval T_s, the estimation objective is to compute a $\hat{\theta}$ that minimizes a scalar quadratic loss function of the innovations or prediction errors :

$$V_N(\theta) = \frac{1}{N}\sum_{k=1}^{N} e^2(t_k, \theta) \tag{3.3.4}$$

where the output error $e(t_k, \theta)$ represents the residual mismatch between the true measured plant output $y(t_k)$ and the deterministic unmodeled-noise simulation

output $\hat{y}(t_k|\theta)$:

$$e(t_k, \theta) = y(t_k) - \hat{y}(t_k|\theta) = y(t_k) - [G(s, \theta)u(t)]_{t=t_k} \tag{3.3.5}$$

Continuous-Time Fitting of Sampled Data

A distinct advantage of the `idproc` estimation paradigm is that the optimization operates directly on continuous-time equations without requiring manual discrete-to-continuous transforms ($d2c$). To match the continuous model $G(s, \theta)$ with the discretely sampled I/O data, the toolbox assumes a specific intersample behavior for the input—typically a Zero-Order Hold (ZOH).

Over any sampling interval $t \in [kT_s, (k+1)T_s)$, the input is assumed constant : $u(t) = u(kT_s)$. Inside the optimization loop, the internal simulation engine computes the exact analytical state-space transition of the continuous system at the discrete time steps :

$$x(kT_s + T_s) = e^{A_c(\theta)T_s}x(kT_s) + \left(\int_{kT_s}^{(k+1)T_s} e^{A_c(\theta)\tau}d\tau\right)B_c(\theta)u(kT_s) \tag{3.3.6}$$

where $A_c(\theta)$ and $B_c(\theta)$ represent the continuous-time parameterized state matrices. This avoids numerical discretization artifacts, such as the generation of non-physical negative real poles or unit-circle clustering issues inherent in high-rate discrete polynomial identification.

3.4 Transfer Function Identification

System identification constructs a mathematical model from experimental input-output data. For electro-pneumatic systems, this step is critical due to nonlinearities from compressible airflow, friction, and valve hysteresis, which complicate purely analytical modelling. The goal is to obtain a linear approximation capturing the dominant dynamics around a chosen operating point for control design.

Given the system's nonlinearities and integrating characteristics, a closed-loop identification approach was adopted, applying a small varying signal

around the operating point. A persistently exciting input, generated by the STM32 microcontroller, ensures all relevant dynamic modes are adequately stimulated. A proportional controller with gain $K_p = 4$ is used initially, with the output amplified externally to match the positioner input range.

The position system is modelled as a second-order transfer function with an open-loop integrator, consistent with the compressibility-driven dynamics of pneumatic actuators. Considering a proportional controller and feedback factor k_f, the closed-loop transfer function $F(s)$ relates the current input to the valve position.[1]

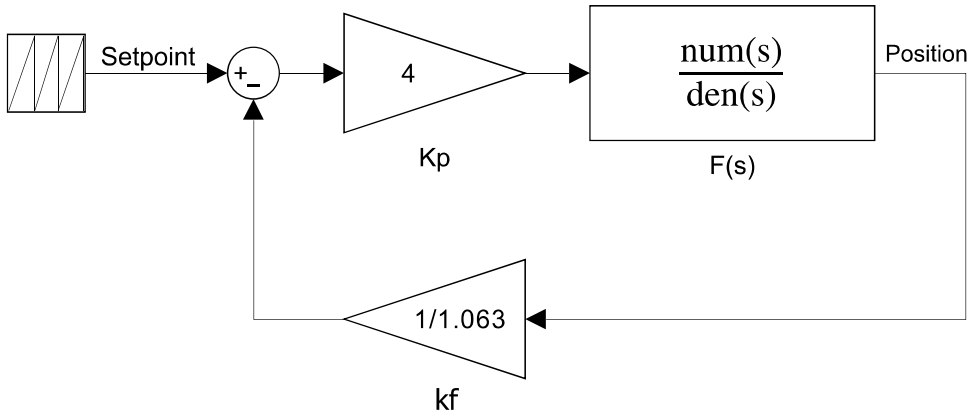


Figure 3.1 – identification close loop

$$F(s) = \frac{1}{k_f} \cdot \frac{1}{\frac{T_1 T_2}{k_p k_s} S^3 + \frac{T_1 + T_2}{k_p k_s} S^2 + \frac{1}{k_p k_s} S + 1} \tag{3.4.1}$$

where T_1 and T_2 are the time constants associated with the open-loop plant dynamics, k_p is the proportional controller gain, and k_s is the static gain of the system. The denominator polynomial defines the characteristic equation of the closed-loop system, whose roots determine the stability and transient behavior of the response.

The step-response obtained experimentally reveals a damped oscillatory behavior. Under the assumption of linear operation around the selected operating point, the third-order characteristic equation associated with $F(s)$ may be re-

presented as the series combination of a damped second-order system and a first-order system. This factored representation is particularly convenient for parameter estimation, as it directly exposes physically meaningful quantities such as the damping ratio and natural frequency, which can be related to the observed transient response characteristics.[1]

$$F(s) = \frac{K}{(1 + 2\zeta\, T_\omega\, s + (T_\omega\, s)^2)\left(1 + T_{p3}\, s\right)} \tag{3.4.2}$$

where K is the system gain, ζ is the damping ratio, T_ω is the natural frequency of the second-order component, and T_{p3} is the time constant of the first-order component. Using MATLAB's System Identification Toolbox, the model parameters were estimated from the recorded experimental datasets by minimizing the prediction error between the model output and the measured system response. The estimation was performed iteratively, with the toolbox employing a nonlinear least-squares algorithm to converge on the parameter values that best fit the observed data. The identified parameters, together with their associated uncertainty bounds, were obtained as follows :

$$\begin{aligned} K &= 1.0629 \pm (3.1305 \times 10^{-5}) \\ \zeta &= 0.60549 \pm 0.00061954 \\ T_\omega &= 0.073032 \pm (7.1261 \times 10^{-5}) \\ T_{p3} &= 0.00016599 \pm (8.2157 \times 10^{-5}) \end{aligned} \tag{3.4.3}$$

The narrow uncertainty bounds associated with each parameter confirm the consistency and reliability of the identification procedure. The damping ratio $\zeta = 0.606$ indicates an underdamped second-order mode, which is consistent with the oscillatory transient observed in the experimental step response. The small value of T_{p3} relative to T_ω suggests that the first-order component contributes a fast dynamic mode that has a limited influence on the overall closed-loop response shape.

Substituting these estimated parameters into the closed-loop transfer function $F(s)$ yields the following numerical expression :

$$F(s) = \frac{1.063}{8.853 \times 10^{-7}\, s^3 + 0.00534\, s^2 + 0.08861\, s + 1} \tag{3.4.4}$$

The feedback factor is then calculated directly from the identified static gain as :

$$k_f = \frac{1}{1.063} = 0.9408 \tag{3.4.5}$$

This value reflects the sensor scaling between the physical valve position and the feedback signal returned to the controller, and is used in subsequent open-loop model derivation.

Figure 3.2 presents a comparison between the measured valve position response and the response generated by the identified model. The same proportional controller gain was employed in both the experimental setup and the simulation to ensure a fair and consistent comparison between the two responses.

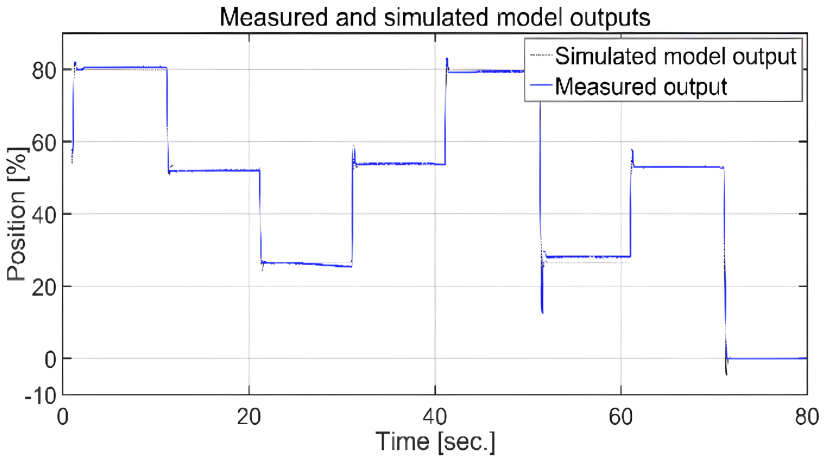


Figure 3.2 – Comparison between measured and simulated position responses [1].

The identified third-order closed-loop model achieved a fit of 94.53% with respect to the estimation data. The Final Prediction Error (FPE) and the Mean Squared Error (MSE) were both equal to 19.67×10^{-5}, indicating a high level of agreement between the model and the experimental data. These metrics collectively confirm that the identified model reproduces the essential dynamic

characteristics of the physical system with sufficient fidelity for the purposes of control design.

Finally, the open-loop transfer function $G(s)$ was derived from the identified closed-loop model by algebraic inversion of the closed-loop expression. Given the closed-loop relationship between the plant $G(s)$, the proportional controller gain k_p, and the feedback factor k_f, the open-loop transfer function can be recovered according to :

$$G(s) = \frac{F(s)}{k_p - k_f k_p F(s)} \tag{3.4.6}$$

Substituting the numerical values of k_p and k_f along with the identified expression for $F(s)$ into the above relation and simplifying yields :

$$G(s) = \frac{3.001 \times 10^5}{s\,(s^2 + 6041\,s + 1.001 \times 10^5)} \tag{3.4.7}$$

The presence of an integrator pole at $s = 0$ in $G(s)$ confirms the integrating nature of the open-loop plant, which is physically consistent with the behavior of a pneumatic positioning system where a constant pressure differential produces a continuously changing position output. The two remaining poles of the denominator correspond to the stable oscillatory dynamics captured by the second-order component of the closed-loop model. This open-loop model serves as the basis for the control design carried out in the following section.

In many practical applications, controller synthesis is first carried out offline using the identified model. This approach allows the controller performance to be evaluated and refined through simulation before implementation on the actual system, thereby reducing commissioning time and minimizing the risk of instability during the tuning phase.[1]

3.5 Validation of Open Loop

3.5.1 Open-Loop Model Validation

Prior to controller synthesis, the fidelity of the identified transfer function model $G(s)$ was assessed through an open-loop hardware validation experiment. The validation was implemented in a dedicated Simulink model deployed on the STM32F303RE target at a sampling period of $T_s = 5\,\text{ms}$, in which the physical pneumatic valve positioner and the discrete transfer function model were driven simultaneously by the same input signal.

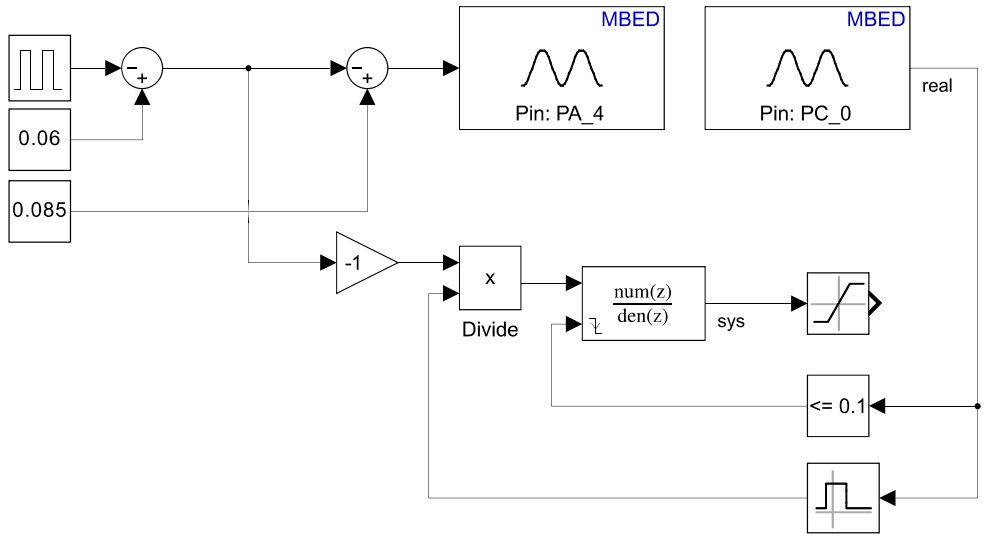


Figure 3.3 – Simulink block diagram used for the model validation

Validation Setup

A periodic square-wave excitation signal was generated using a Simulink Pulse Generator block, sweeping the valve between two operating positions across the full stroke range. The command signal was applied to the physical actuator via the analog output (pin PA_4) and in parallel to the discretized plant model, obtained by converting $G(s)$ to its discrete-time equivalent using zero-order hold (ZOH) at $T_s = 5\,\text{ms}$. The measured position of the physical valve was acquired via the analog input (pin PC_0) at the same sampling rate, and both

the measured and simulated responses were logged to the MATLAB workspace via `To Workspace` blocks for post-processing comparison.

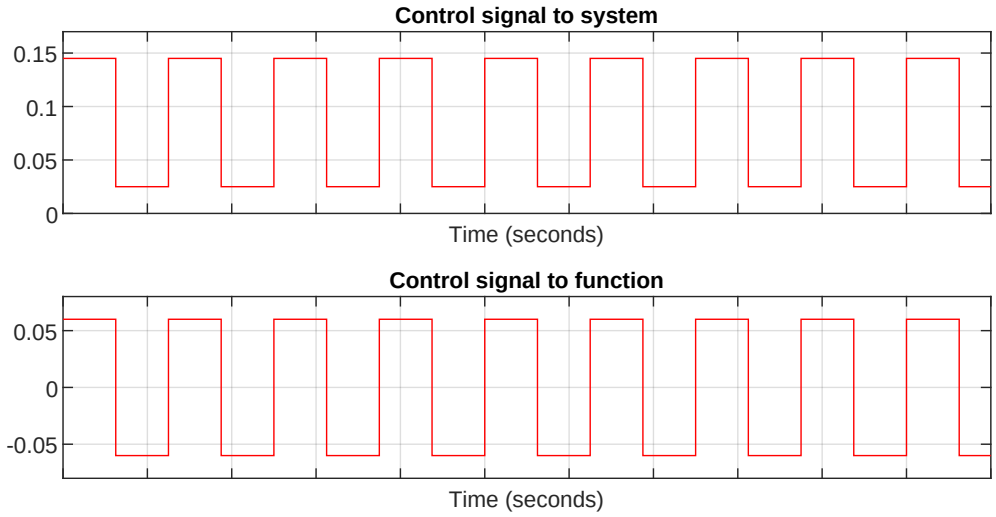


Figure 3.4 – Open loop controle signals

Validation Results

Figure 3.5 presents the overlay of the measured and simulated position responses over a duration of 220 seconds. The two signals exhibit close agreement throughout the experiment, confirming that the identified third-order transfer function captures the dominant dynamic behaviour of the physical system with acceptable accuracy. The slight discrepancies observed during the transient phases — particularly at the rising and falling edges — are attributed to nonlinear friction effects and pneumatic hysteresis inherent to the electro-pneumatic actuator, which are not captured by the linear nominal model.

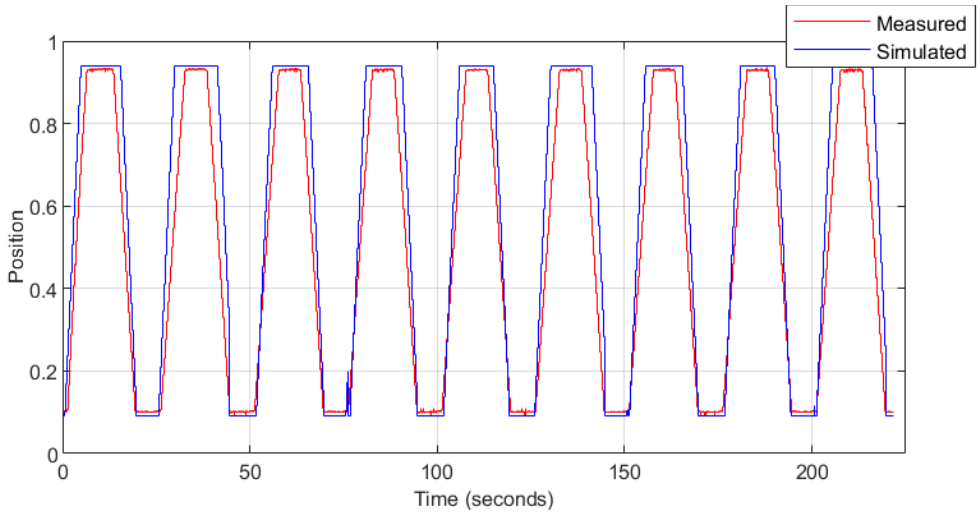


Figure 3.5 – Open-loop model validation : measured vs. simulated position responses

These residual modeling errors constitute the unmodeled dynamics and parametric uncertainties that motivate the use of H_∞ robust control in Chapter, where the controller is synthesized to guarantee closed-loop stability and performance despite such discrepancies between the nominal model and the physical system. The Mean Squared Error (MSE) between the measured and simulated outputs was computed as :

$$\text{MSE} = \frac{1}{N}\sum_{k=1}^{N}\left(y(k) - \hat{y}(k)\right)^2 = 0.0160 \tag{3.5.1}$$

The MSE quantifies the average squared deviation between the model output and the real system response over the entire validation window. A value of 0.0160 indicates that the identified transfer function reproduces the system behavior with a low prediction error, given that the position signal operates over a normalized range of $[0, 1]$. The residual error is primarily concentrated at transient intervals and is consistent with the nonlinear characteristics of the pneumatic actuator, particularly the dead zone effect, which the linear model does not account for. Overall, this result confirms a satisfactory level of accuracy and validates the identified model as a suitable basis for robust controller design.

3.6 Conclusion

This chapter presented the identification and open-loop validation of a mathematical model for the electro-pneumatic valve positioning system. A closed-loop identification approach was adopted to accommodate the integrating and nonlinear characteristics of the plant, with a proportional controller of gain $K_p = 4$ used to stabilise the system during data acquisition. The experimental step response was fitted to a third-order closed-loop transfer function, achieving a model fit of 94.53% with an FPE and MSE of 19.67×10^{-5}, confirming the reliability of the estimated parameters.

The open-loop transfer function $G(s)$, recovered by algebraic inversion of the closed-loop model, exhibits an integrator pole at $s = 0$ consistent with the physical behaviour of a pneumatic actuator, alongside a stable oscillatory second-order mode. Open-loop hardware validation against periodic square-wave excitation confirmed close agreement between the simulated and measured responses, with residual discrepancies attributed to nonlinear friction and pneumatic hysteresis not captured by the linear nominal model. These unmodelled dynamics and parametric uncertainties motivate the robust control strategy developed in the subsequent chapter.

3.7 Fixed-Structure H_∞ Optimal Tuning via `hinfstruct`

3.7.1 Introduction

Modern industrial control design demands a rigorous balance between deterministic performance metrics (such as tracking accuracy and regulation bandwidth) and robust stability margins against plant parameter variations. While classical H_∞ optimal control theory offers unmatched mathematical guarantees regarding robust performance, it traditionally yields full-order controllers. The dynamic order of an unconstrained H_∞ controller matches or exceeds that of the augmented open-loop generalized plant, rendering its implementation computationally prohibitive and structurally incompatible with standard industrial hardware infrastructures.

To reconcile advanced robust control theory with industry-standard hardware constraints, this work utilizes the fixed-structure H_∞ synthesis framework via MATLAB's `hinfstruct` engine. This methodology restricts the controller topology *a priori* to a standard Parallel Proportional-Integral-Derivative (PID) form. Rather than solving an unconstrained state-space optimization, the algorithm computes the real-valued controller gains natively within a frequency-domain loop-shaping framework, bypassing the need for subsequent order reduction or heuristic curve-fitting. [18]

3.7.2 Theoretical Framework and Generalized Plant Synthesis

The optimization problem is formulated by isolating the parameterized controller $K(s)$ from an augmented open-loop generalized plant $P(s)$ utilizing a lower Linear Fractional Transformation (LFT) framework.

The generalized plant $P(s)$ encapsulates the nominal plant dynamics $G(s)$ combined with frequency-dependent weighting filters designed to shape the closed-loop frequency response. The system signals are explicitly partitioned into three operational vector spaces :

1. **Exogenous Inputs (w) :** Comprising the reference command (c), input plant disturbance (b_u), and measurement channel noise (b_y).
2. **Regulated Outputs (z) :** Bounding the weighted tracking error (z_e), weighted control actuation penalty (z_u), and weighted plant output (z_y).
3. **Internal Controller Interface (u, e) :** The synthesized control effort (u) and the tracking error feedback (e).

The closed-loop block connectivity is mathematically defined by the following internal algebraic summing junctions :

$$e = c - y_{\text{meas}} \tag{3.7.1}$$

$$y_{\text{meas}} = y + W_{yb} \cdot b_y \tag{3.7.2}$$

$$u_{\text{plant}} = u + W_b \cdot b_u \tag{3.7.3}$$

Correspondingly, the tracking metrics map to the regulated vector via the

frequency-dependent filtering arrays :

$$z_e = W_e \cdot e, \quad z_u = W_u \cdot u, \quad z_y = W_y \cdot y \tag{3.7.4}$$

By packing these channels, the open-loop interconnection is matrix-defined via the transfer function block equation :

$$\begin{bmatrix} z_e \\ z_u \\ z_y \\ \hline e \end{bmatrix} = P(s) \begin{bmatrix} c \\ b_u \\ b_y \\ \hline u \end{bmatrix} = \begin{bmatrix} P_{11}(s) & P_{12}(s) \\ P_{21}(s) & P_{22}(s) \end{bmatrix} \begin{bmatrix} w \\ \hline u \end{bmatrix} \tag{3.7.5}$$

By executing a lower LFT over the structural parameter space $\theta = \{K_p, K_i, K_d\}$, the closed-loop map $T_{zw}(s)$ is evaluated as :

$$F_l(P, K) = T_{zw}(s) = P_{11}(s) + P_{12}(s)K(s)\left(I - P_{22}(s)K(s)\right)^{-1} P_{21}(s) \tag{3.7.6}$$

The optimization problem seeks to minimize the worst-case energy amplification across all frequencies [18]

$$\min_{\theta \in \mathbb{R}^3} \|T_{zw}(s, \theta)\|_\infty = \min_{\theta \in \mathbb{R}^3} \sup_{\omega \in \mathbb{R}} \sigma_{\max}\left(T_{zw}(j\omega, \theta)\right) \tag{3.7.7}$$

3.7.3 Application to the Proposed Model

The structural methodology is applied to an second-order model with an integrator

$$G(s) = \frac{300100}{s(s^2 + 6041s + 1.001 \times 10^5} \tag{3.7.8}$$

Weighting Boundary Configuration

To construct $P(s)$, frequency-shaping performance blocks are selected to define loop boundaries :

— **Tracking Sensitivity Boundary (W_e) :** Formulated as a low-pass profile

to shape $S = (1 + GK)^{-1}$:

$$W_e(s) = \frac{\frac{s}{1.4} + 0.5}{s + 0.005} \tag{3.7.9}$$

This limits low-frequency tracking mismatch to an error floor $A = 0.01$ (1%) up to a target operating bandwidth $\omega_b = 0.5$ rad/s, under a peak sensitivity limit $M = 1.4$.

— **Actuator and Robustness Filters (W_u, W_y) :** The control output penalty is scaled to $W_u = 0.15$ to mitigate high-frequency actuator chatter (KS). The output complementary stability envelope is fixed via $W_y = 1.2$ to bound T.

— **Disturbance and Noise scaling (W_b, W_{yb}) :** Plant input disturbance scaling is defined as $W_b = 3.5$, and the high-frequency measurement sensor noise floor is weighted at $W_{yb} = 0.1$.

The structural controller block is hard-coded to a parallel layout with a static high-frequency derivative filter pole $T_f = 0.01$ s ($N = 100$ rad/s) to suppress numerical high-frequency derivative amplification :

$$K(s) = K_p + \frac{K_i}{s} + \frac{K_d s}{0.01s + 1} \tag{3.7.10}$$

Synthesis Optimization Results

Following optimization execution across 20 randomized starting points, the algorithm converged on a mathematically optimal parameter vector θ^*. The derived structural PID controller parameter values are :

$$K_p = 3.000000, \quad K_i = 0.537500, \quad K_d = 0.046600 \tag{3.7.11}$$

This parameter vector yields the final optimized control law mapping :

$$K_{\text{opt}}(s) = 3 + \frac{0.5375}{s} + \frac{0.0466s}{0.01s + 1} \tag{3.7.12}$$

The achieved structured infinity norm satisfies $\gamma_{\text{opt}} \leq 1$, confirming that all competing loop-shaping parameters—including tracking accuracy, disturbance

rejection boundaries, and sensor noise margins—are optimized simultaneously within a singular, robustly stable framework.

3.7.4 Simulation Results

The simulated position tracking results for the structured H_∞- PID controller are shown in the Figure 3.6 below.

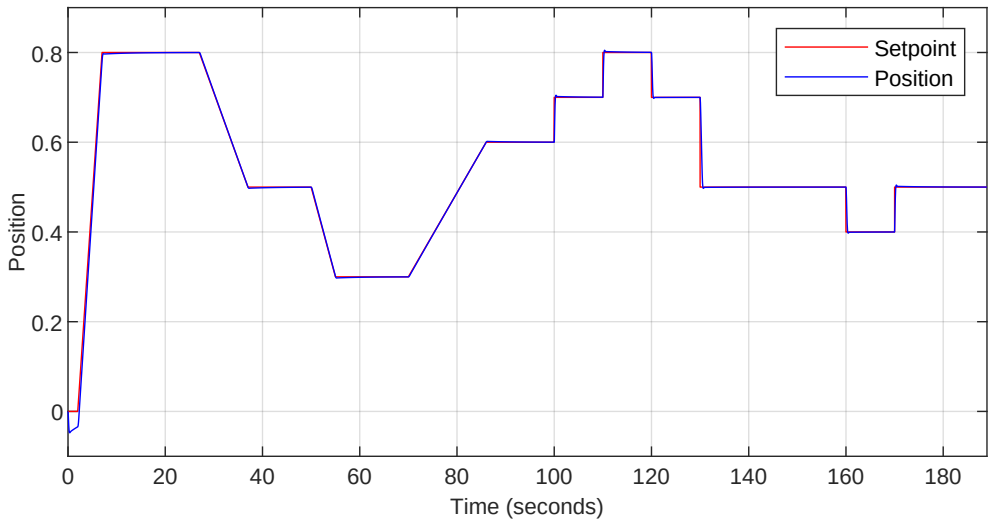


Figure 3.6 – Simulation results of position

3.7.5 Experimental Results of the H_∞-Tuned PID Controller

The H_∞-synthesized PID controller was deployed on the STM32F303RE and tested in real time on the proportional pneumatic valve positioner. Figure **??** presents the measured closed-loop response of the system, comparing the actual valve position against the commanded reference setpoint.

The experimental results demonstrate that the controller tuned via the `hinfstruct` procedure achieves accurate setpoint tracking with a fast settling time and negligible steady-state error. The robustness margins enforced during the H_∞ synthesis translate directly to the physical bench, where the positioner maintains stable behavior and effective disturbance rejection despite the nonlinearities and friction inherent to the pneumatic actuator. This confirms

that the performance predicted in simulation is preserved after embedded deployment.

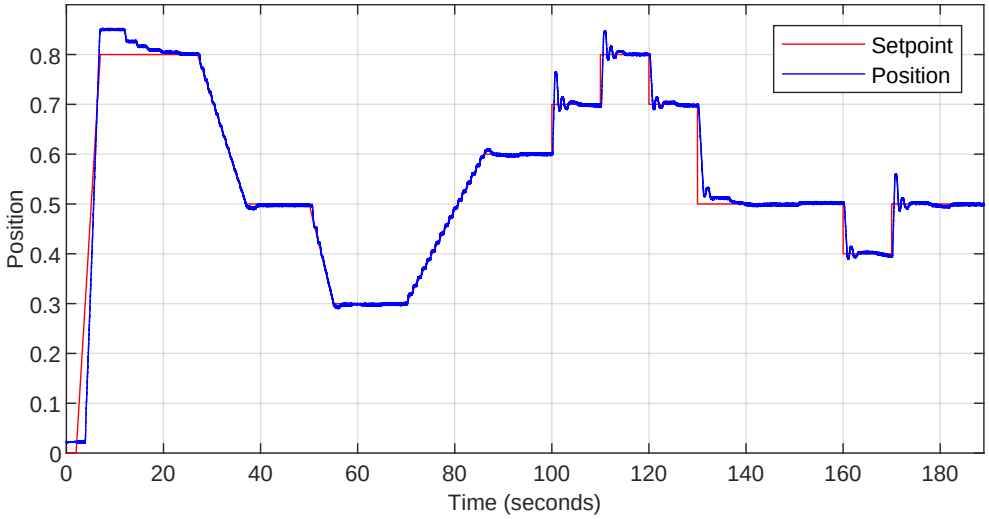


Figure 3.7 – Real results of position

3.8 Conclusion

This chapter presented the identification of a third-order closed-loop transfer function for the electro-pneumatic valve positioner using MATLAB's 'idproc' framework, achieving a 94.53% fit. The open-loop plant model, recovered by algebraic inversion, confirmed the expected integrator dynamics of the pneumatic actuator and was validated against hardware with an MSE of 0.0160. A fixed-structure H PID controller was then synthesized via 'hinfstruct', yielding optimal gains that satisfy all loop-shaping constraints within a unified robust framework. Both simulation and experimental deployment on the STM32F303RE confirmed accurate setpoint tracking, fast settling, and effective disturbance rejection, validating the identified model and the synthesized controller as a reliable foundation for robust pneumatic valve positioning.

General Conclusion

This thesis has presented a comprehensive investigation into the modeling, system identification, and foundational control framework of an electro-pneumatic valve positioning system, progressing systematically from fundamental mechanical principles to a validated mathematical representation suitable for advanced control synthesis. The first chapter established the technical groundwork by examining industrial valves as critical final control elements within fluid power networks. A systematic review of valve classifications by function, mechanical motion, and dimensional scale revealed the diverse architectures employed across modern process industries, ranging from gate and globe valves to ball, butterfly, and eccentric plug configurations. The chapter further traced the historical evolution of fluid control technology from ancient irrigation systems to contemporary smart actuation, and culminated in a detailed analysis of pneumatic actuators and cylinders. The comparative study of single-acting and double-acting configurations highlighted the inherent trade-offs between fail-safe integrity, force density, and bidirectional control capability that govern actuator selection in industrial practice. Building upon this foundation, the second chapter examined the valve positioner as the closed-loop intermediary that compensates for mechanical non-idealities such as stiction, deadband, and hysteresis. The evolutionary trajectory of positioners — from early mechanical linkages and force-balance pneumatic devices to modern digital and smart positioners equipped with on-board diagnostics — was traced in detail, with particular focus on the analog EP100 architecture as a representative case study. The chapter further developed analytical transfer-function models

for the double-acting pneumatic cylinder, the directional control valve, and the solenoid coil assembly, establishing the mathematical scaffolding required for subsequent identification and control design. The third chapter addressed the inherent nonlinearities of the physical plant — including compressible airflow, mechanical friction, and valve hysteresis — through a closed-loop system identification approach. A persistently exciting input signal generated by an STM32 microcontroller stimulated the dominant dynamic modes of the system, enabling the estimation of a third-order closed-loop transfer function with narrow uncertainty bounds.

Collectively, these three chapters provide a rigorous foundation that transitions from passive mechanical components to a validated mathematical representation of the electro-pneumatic positioning loop. The residual discrepancies between the linear nominal model and the physical system — attributed to unmodelled nonlinear friction and pneumatic hysteresis — constitute the parametric uncertainties that motivate the development of a robust control strategy in subsequent work. This structured methodology contributes to the advancement of automated process instrumentation and establishes a clear pathway toward the design of high-fidelity, intelligent valve control systems for demanding industrial applications.

References

[1] S. M. E. E. Abdi, Y. Bouderbala, H. Bensadek, and L. Merad, "Advanced control for double acting pneumatic valve positioning system," *Electrotehnica, Electronica, Automatica (EEA)*, vol. 72, no. 4, 2024, confirm final page numbers. [Online]. Available : https://doi.org/10.46904/eea.25.73.3.1108016

[2] American Society of Mechanical Engineers, "ASME B16.34-2020 : Valves — Flanged, Threaded, and Welding End," ASME Standard, New York, NY, USA, 2020. [Online]. Available : https://www.asme.org/codes-standards/find-codes-standards/b16-34-valves-flanged-threaded-welding-end

[3] American Petroleum Institute, "API Standard 594 : Check Valves — Flanged, Lug, Wafer, and Butt-welding," API Standard, 8th Edition, Washington, D.C., USA, 2017.

[4] F. M. White, *Fluid Mechanics*, 8th ed. McGraw-Hill Education, 2015. [Online]. Available : https://www.mheducation.com/highered/product/fluid-mechanics-white.html

[5] International Society of Automation, "ANSI/ISA-75.25.01-2000 : Test Procedure for Control Valve Response Measurement from Step Inputs," ANSI/ISA Standard, 2000. [Online]. Available : https://webstore.ansi.org/standards/isa/ansiisa7525012000

[6] American Society of Mechanical Engineers, "ASME PTC 19.5 : Flow Measurement," ASME Performance Test Code, 2022. [Online].

Available : https://www.asme.org/codes-standards/find-codes-standards/flow-measurement

[7] International Society of Automation, "ANSI/ISA-96.01.01 : Terminology Used for Valve Actuators," ANSI/ISA Standard, 2019. [Online]. Available : https://www.isa.org/products/ansi-isa-96-01-01-2019-valve-actuator-terminology

[8] ——, "ANSI/ISA-75.05.01-2000 (R2005) : Control Valve Terminology," ANSI/ISA Standard, 2000. [Online]. Available : https://webstore.ansi.org/standards/isa/ansiisa7505012000r2005

[9] K. J. Åström and T. Hägglund, *Advanced PID Control*. ISA — The Instrumentation, Systems, and Automation Society, 2006. [Online]. Available : https://portal.research.lu.se/en/publications/advanced-pid-control/

[10] International Society of Automation, "ANSI/ISA-50.00.01 : Compatibility of Analog Signals for Electronic Industrial Process Instruments," ANSI/ISA Standard, 1975. [Online]. Available : https://webstore.ansi.org/standards/isa/ANSIISA5000011975R2012

[11] International Electrotechnical Commission, "IEC 60534-1 : Industrial-Process Control Valves — Part 1 : Control Valve Terminology and General Considerations," IEC Standard, 2023. [Online]. Available : https://webstore.iec.ch/en/publication/32585

[12] D. M. Considine, *Process/Industrial Instruments and Controls Handbook*. McGraw-Hill, 1993. [Online]. Available : https://books.google.dz/books?id=1d9TAAAAMAAJ

[13] International Electrotechnical Commission, "IEC 60534-6-1 : Industrial-Process Control Valves — Part 6-1 : Mounting Details for Attachment of Positioners to Control Valves," IEC Standard, 1997. [Online]. Available : https://webstore.iec.ch/publication/2469

[14] D. McCloy and H. R. Martin, *Control of Fluid Power : Analysis and Design*, 2nd ed. Chichester, UK : Ellis Horwood, 1980. [Online]. Available : https://catalog.hathitrust.org/Record/000720935

[15] S. N. Joshi, "Mechatronics and manufacturing automation, module 6, lecture 5 : Pneumatic controllers," National Programme on Technology

Enhanced Learning (NPTEL), IIT Guwahati, 2012. [Online]. Available : https://archive.nptel.ac.in/courses/112103174/

[16] C. G. Proudfoot, "Principles and practice of automatic process control : Carlos a. smith and armando b. corripio," *Automatica*, vol. 23, no. 3, p. 414, 1987.

[17] M. N. Muftah, W. L. Xuan, and A. A. M. Faudzi, "ARX, ARMAX, Box-Jenkins, Output-Error, and Hammerstein models for modeling intelligent pneumatic actuator (IPA) system," *Journal of Integrated and Advanced Engineering (JIAE)*, vol. 1, no. 2, pp. 81–88, 2021. [Online]. Available : https://doi.org/10.51662/jiae.v1i2.18

[18] P. Apkarian and D. Noll, "Nonsmooth h synthesis," *IEEE Transactions on Automatic Control*, vol. 51, no. 1, pp. 71–86, 2006.